

COMBINED OPERATION AND STAGING FOR THE FCC-ee COLLIDER*

M. Benedikt[†], B. Holzer, E. Jensen, R. Tomas, J. Wenninger, F. Zimmermann, CERN, Geneva Switzerland; A. Bogomyagkov, E. Levichev, D. Shatilov, BINP, Novosibirsk, Russia
U. Wienands, SLAC, USA; K. Ohmi, K. Oide, KEK, Tsukuba, Japan

Abstract

FCC-ee is a proposed high-energy electron positron circular collider that might initially occupy the 100-km FCC tunnel which would eventually house the 100 TeV FCC-hh hadron collider. The parameter range for the e^+e^- collider is large, operating at c.m. energies from 90 GeV (Z -pole) to 350 GeV ($t\bar{t}$ production) with beam currents ranging between 1.5 A and 7 mA, at fixed synchrotron radiation power of 50 MW per beam, and the radiative energy loss varying from about 30 MeV/turn to 7500 MeV/turn. This presents challenges for the radiofrequency (rf) system due to the varying rf voltage requirements and beam loading conditions. In this paper we present a possible gradual evolution of the FCC-ee complex by step-wise expansion, and possibly reconfiguration, of the superconducting rf system and of the optics. The performance attainable at each step is discussed, along with possible advantages and drawbacks.

PHYSICS GOALS AND ENERGIES

The highest priority of a potential future e^+e^- collider in the 100-km FCC tunnel is Higgs production at a centre-of-mass energy of about 240 GeV corresponding to the peak rate of $e^+e^- \rightarrow ZH$ events. The second FCC-ee priority is running on the Z pole (91 GeV c.m.) with exceptionally high luminosity in order to generate 10^{12} – 10^{13} Z 's over a couple of years. Further FCC-ee collision energies will be at the $t\bar{t}$ threshold (~ 350 GeV c.m.), at the WW threshold, and possibly, with energy monochromatization, on the $e^+e^- \rightarrow H$ resonance (~ 125 GeV). The baseline physics program assumes no longitudinal polarization. However, scaling from LEP experience, some transverse polarization of non-colliding bunches is expected at the Z and up to the WW threshold, which can be used for precise calibration of the beam energy.

PARAMETERS AND OPERATION MODES

The number of FCC-ee interaction points (IPs) could be 2 or 4. A model used to describe the performance of LEP [1] suggests that with two collision points the maximum beam-beam tune shift and the luminosity per IP could be about 40% higher than with four collision points. However, the collision conditions for many of the FCC-ee scenarios are rather different from those at LEP. Preliminary

weak-strong simulations for FCC-ee indicate a weaker dependence on the number of IPs, i.e. only a 10–20% gain in the maximum beam-beam tune shift at 240 GeV c.m. with 2 instead of 4 IPs [2] and even less (or no) gain at 91 GeV c.m. However, our further discussion assumes two IPs.

For constant synchrotron radiation power, e.g. 50 MW per beam, at lower beam energy the beam current increases as the inverse fourth power of energy. The much higher beam current at lower energy implies a correspondingly increased number of bunches.

Indeed, the requirements on the rf system differ substantially at low and high energies. On the Z pole the beam current is about 1.5 A, but the energy loss per turn only some 30 MeV and the rf voltage required is moderate. The cavity impedance is a concern for this mode of operation [3]. In consequence, the smallest number of cavities which can still provide 2×50 MW to the beams would be desired. Conversely, when running at the ZH peak or at the $t\bar{t}$ threshold the beam current is much lower, 30 or 7 mA, but the energy loss per turn amounts to 1.7 or 7.6 GeV, respectively, calling for a total rf voltage of up to 11 GV. Because of the lower beam current and higher beam energy, the cavity impedance is less of a concern here. Therefore, a staging where cavity modules are installed in steps appears natural.

The geometric emittance from the arcs scales as $\theta_b^3 \gamma^2$ [4], where θ_b denotes the bending angle per arc cell and γ the Lorentz factor. The natural emittance decrease at lower energy can be counteracted by choosing longer optical cells in the arcs. The baseline parameter set of FCC-ee [5] assumes a 50-m arc FODO cell length, required for ZH and $t\bar{t}$ running, a 100 m cell length for the WW threshold and a 300-m cell length at the Z pole [6]. The increased cell length at lower energies allows for the geometric emittance to stay roughly constant or even to increase, at similar bunch charge, in order for the beam-beam tune shift to remain at, or below, the expected energy-dependent limit [1].

If the cell length is held constant, equal to 50 m, at the lower beam energies the emittance shrinks substantially. In this case the beam-beam tune shifts can still be kept under control, however, with the help of a large crossing angle, complemented by crab-waist sextupoles. In such a crab-waist scenario, the luminosity at the Z pole is about an order of magnitude higher than for the baseline [7]. The low-emittance crab-waist running implies extremely small vertical emittance values. Table 1 compares some example parameters (based on analytical calculations, and not fully optimized) for the proposed schemes at two beam energies.

It may be possible to further reduce the rf voltage, much

* This work was supported in part by the European Commission under the FP7 Capacities project EuCARD-2, grant agreement 312453.

[†] michael.benedikt@cern.ch

below the values shown in the table, in order to lengthen the bunches. E.g., by choosing 200 or 80 MV instead of 400 MV at the Z pole, the rms bunch length for the crab-waist scheme without beamstrahlung (non-colliding beams) would exceed 1.6 or 2.5 mm, respectively. Longer bunches would reduce the excitation of higher-order modes and the energy-loss factor for the rf cavities.

Table 1: Parameters for FCC-ee running at 91 GeV (Z) and 240 GeV (ZH) centre-of-mass energy, considering two IPs, a ring circumference of 100 km, and an rf frequency of 400 MHz. ‘CW’ refers to crab waist, ‘SR’ to synchrotron radiation, ‘BS’ to beamstrahlung. The bunch length with beamstrahlung is calculated by solving an approximate self-consistent analytical equation [13]. The baseline and crab-waist parameters roughly correspond to those proposed in Refs. [5] and [7] [modified so as to correspond to the 120/175-GeV arc optics parameters of Ref. [5]], respectively.

beam energy [GeV]	45.5		120	
	base	CW	base	CW
beam current [A]	1.45	1.45	0.03	0.03
energy loss / turn [GeV]	0.03	0.03	1.67	1.67
rf voltage [GV]	2.5	0.4	5.5	3.6
mom. comp. [10^{-5}]	18	0.5	0.5	0.5
# bunches / beam	13k	60k	1046	474
N_b [10^{11}]	2.4	0.5	0.6	1.3
β_x^* [m]	0.5	0.5	0.5	0.5
β_y^* [mm]	3	1	1	1
ϵ_x [nm]	29	0.13	0.94	0.94
ϵ_y [pm]	60	1	2	1
σ_z (SR only) [mm]	3.3	1.0	1.6	2.1
σ_z (with BS) [mm]	3.8	2.8	1.8	2.6
θ_c [mrad]	11	30	11	30
b.-b. param. ξ_x /IP	0.04	0.07	0.10	0.06
b.-b. param. ξ_y /IP	0.07	0.18	0.11	0.18
Piwinski angle	0.17	5.3	0.46	1.8
lum./IP [$10^{34} \text{ cm}^{-2} \text{ s}^{-1}$]	27	247	7	11

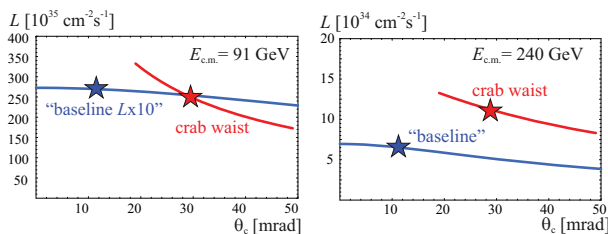


Figure 1: Luminosity per IP vs. full crossing angle. The stars indicate the operation points of Table 1.

Achieving the target emittance values may be challenging, given the size of the ring (with misalignments), the presence of beam-beam collisions, the effects of synchrotron radiation etc. In particular, for the crab waist scheme the 30-mrad crossing angle can lead to signif-

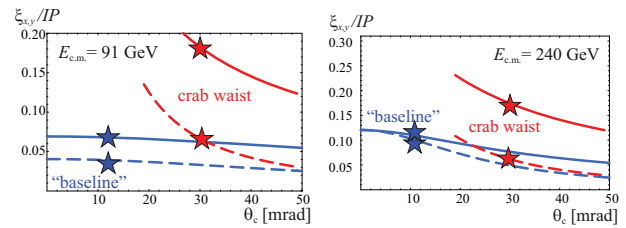


Figure 2: Beam-beam parameter per IP vs. full crossing angle. Solid lines: ξ_y , dashed: ξ_x . The stars indicate the operation points of Table 1.

icant synchrotron radiation, and resulting vertical emittance blow up, in the body and fringe fields of the detector solenoid and antisolenoids of the interaction region [8, 9, 10, 11, 12].

Figure 1 shows the luminosity as a function of the full crossing angle for parameters corresponding to the baseline [5] and for the low-emittance crab-waist scheme [7]. For the latter we consider only crossing angles from 20 mrad onwards, where the Piwinski angle is sufficiently large. In the baseline, the (smaller) crossing angle causes a negligible loss of geometric luminosity, but it may lead to an undesired excitation of synchro-betatron resonances, which could be mitigated by crab cavities [14].

Figure 2 presents the corresponding beam-beam parameters. Ideal would be a final-focus system which can accommodate both the baseline and a crab-waist scheme. In order to operate the latter at crossing angles below 30 mrad, say at 20 mrad, we should decrease the bunch charge and increase the number of bunches, in order to obtain acceptable tune shifts

GRADUAL EVOLUTION AND STAGING

The low-emittance crab-waist scheme is most interesting at the Z pole, where the luminosity gain is maximum [7]. Table 2 shows three possible stages at this energy, illustrating the transition from less challenging parameters to a crab-waist scheme. The transition is characterized by decreasing emittances (corresponding to FODO cell lengths of 300 m, 100 m and 50 m, respectively), reduced β_y^* , increasing number of bunches, and growing luminosity. The constant crossing angle of 20 mrad was chosen as an intermediate value between the two scenarios of Table 1, where the Piwinski angle is still larger than 2 at the smallest horizontal emittance considered. The RF voltage of only 0.2 GV may allow for a total cavity impedance compatible with the desired high beam current. The table illustrates that by reducing the arc emittance and simultaneously changing the bunch filling pattern the luminosity can be increased by an order of magnitude. Therefore, as the orbit control and emittance tuning of FCC-ee improve, operational stages on the Z pole could, or should, proceed towards shorter arc cell lengths.

The rf system naturally lends itself to staging, i.e., it can

Table 2: Example stages at 91 GeV c.m., with a constant crossing angle of 20 mrad and varying emittance. The luminosity numbers are still to be confirmed by simulations.

beam energy [GeV]	45.5		
beam current [A]	0.7 (1.45)	1.45	1.45
rf voltage [GV]	0.2	0.2	0.2
arc cell length [m]	300	100	50
mom. comp. [10^{-5}]	18	2	0.5
β_y^* [mm]	3	1	1
# bunches	6k (13k)	54k	130k
N_b [10^{11}]	2.4	.55	0.23
ϵ_x [nm]	29	3.5	0.13
ϵ_y [pm]	60	7	2
σ_z (SR only) [mm]	11.7	2.8	1.4
σ_z (with BS) [mm]	11.9	3.1	2.3
b.-b. param. ξ_x / IP	0.02	0.05	0.09
b.-b. param. ξ_y / IP	0.05	0.06	0.10
Piwinski angle	0.98	0.74	2.91
lum./IP [10^{34} cm $^{-2}$ s $^{-1}$]	8 (15)	68	134

be expanded in steps, with increasing rf power and rising maximum voltage. In addition, when transiting from a beam energy of 120 GeV to 175 GeV, it may be attractive to reconfigure the rf system and to share it between the two beams, so as to double the rf voltage available for either beam (keeping the rf power per beam constant). This reconfiguration avoids doubling the number of rf cavities, possibly a substantial cost saving. The sharing of cavities by the two beams is possible thanks to the small number of bunches at $t\bar{t}$ running (75 bunches per beam).

Combining the evolutions of IR, arc optics and rf system, we can consider, e.g., the following four operational stages:

1. half the rf system: half the number cavities with half nominal rf power and half the maximum voltage; large emittance arc optics; $\beta_y^* = 3$ mm; initial running at the Z , WW and ZH ;
2. full rf system: full power and voltage; intermediate optics (100 m cell length); $\beta_y^* = 1$ mm; higher-luminosity running at the Z , WW and ZH ;
3. full rf system: full power and voltage; lowest emittance arc optics (shortest cell length); high-luminosity running at the Z , WW and ZH ; possible operation on the H resonance with mono-chromatization [15];
4. reconfigured rf system: high-luminosity running at $t\bar{t}$ and, possibly, ZH .

Table 3 summaries the luminosity performance for the different energies. Within each stage, the β^* , the arc cell length and the rf power are kept the same for all collision energies, which should facilitate switching between these energies. Successive stages become ever more challenging, as the cell length and the IP beta function are pushed down (higher chromaticity), and as more rf cavities are seen by the beam (higher impedance).

The possibility of a special run with mono-chromatic collisions [15] on the $e^+e^- \rightarrow H$ resonance is also indicated in Table 3. A large horizontal IP dispersion (e.g. $D_x^* \approx 2$ m) would yield a relative c.m. energy spread of $\sim 10^{-5}$, i.e. 3 times smaller than the standard-model width of the Higgs boson. The luminosity value quoted with a question mark in Table 3 accounts for the dispersive contribution to the horizontal IP beam size, but does not consider any horizontal emittance growth due to the combined effect of IP dispersion and beamstrahlung beyond a factor ~ 2 margin included in the FCC-ee optics design. The generation of the large IP dispersion (in a dedicated IP?) as well as the possibly large emittance growth caused by beamstrahlung with $D_x^* \neq 0$ [16] requires further investigation.

Table 3: Example operational stages of FCC-ee. The total crossing angle is held constant, equal to $\theta_c = 20$ mrad.

stage	1	2	3	4
$V_{rf,max}$ / beam [GV]	2.7	5.5	5.5	11
P_{rf} / beam [MW]	25	50	50	50
β_y^* [mm]	3	1	1	1
arc cell length [m]	300	100	50	50
L/IP [10^{34} cm $^{-2}$ s $^{-1}$]				
91 GeV (Z)	8	68	134	—
125 GeV (H)	—	—	27?	—
160 GeV (WW)	7	22	31	—
240 GeV (ZH)	0.1	3.4	6.8	10?
350 GeV ($t\bar{t}$)	—	—	—	2.1

CONCLUSIONS

Staging the FCC-ee could save time or money. A staged construction could also improve the performance, e.g. by minimizing the impedance at low energy. Staging might as well profit from growing operational experience. Many types of staging are possible, e.g. a stage could be equal to the operation at a single beam energy — an obvious option, which we have not considered in this paper.

As an illustration of a more complex scheme, we have presented a combined staging scenario for the collider-ring optics and rf systems, which allows for interesting physics in each stage, and which renders the machine operation and optics tuning gradually more challenging. In this example, the crossing angle is held constant for all stages and energies. Between stages 1 and 2 additional rf units are installed, e.g. during an annual winter shutdown. If helpful also arc quadrupoles could be added in the stops between stages, since, e.g. the first stage requires 6 times fewer quadrupoles in the arc than the final stage. The step from stage 3 to stage 4 requires a reconfiguration of the rf system, e.g. transverse movements of the rf cavities by tens of centimetres, plus, probably, the installation of electrostatic combiners and separators at the entrance and exit of each rf straight section.

REFERENCES

- [1] R. Assmann, K. Cornelis, “The Beam-Beam Interaction in the Presence of Strong Radiation Damping,” Proc. EPAC2000 Vienna, p. 1187.
- [2] K. Ohmi, “Beam-Beam Studies for New Parameters of FCC,” FCC-ee video meeting, 16 March 2015.
<http://indico.cern.ch/event/378585/>
- [3] M. Migliorati, “Impedance and Collective Effects,” FCC Week 2015, Washington DC.
<http://indico.cern.ch/event/340703/session/81/contribution/158/material/slides/0.pdf>
- [4] L.C. Teng, “Minimizing the Emittance in Designing the Lattice of an Electron Storage Ring,” Fermilab TM-1269 (1984).
- [5] J. Wenninger et al., “Future Circular Collider Study — Lepton Collider Parameters,” FCC-ACC-SPC-0003 rev. 2.0 (2014).
- [6] B. Haerer et al., “First Considerations on Beam Optics and Lattice Design for the Future Electron-Positron Collider FCC-ee”, IPAC 2015, these proceedings.
- [7] A. Bogomyagkov, E. Levichev, and D. Shatilov, “Beam-Beam Effects Investigation and Parameter Optimization for Circular e^+e^- Collider TLEP to study the Higgs Boson,” Phys. Rev. ST Accel. Beams 17, 041004 (2014).
- [8] V. Telnov, “Dilution of the Vertical Beam Emittance in the Crab-Waist Scheme due to a Detector Field,” FCC-ee video meeting, 19 January 2015.
<http://indico.cern.ch/event/360323>
- [9] S. Sinyatkin, “Preliminary Model of the Solenoidal Fields in FCC-ee,” FCC-ee video meeting, 16 March 2015.
<http://indico.cern.ch/event/378585>
- [10] A. Bogomyagkov et al., Interaction Region of the Future Electron-Positron Collider FCC-ee”, IPAC 2015, these proceedings.
- [11] R. Martin et al., ”Status of the FCC-ee Interaction Region Design”, IPAC 2015, these proceedings.
- [12] H. Burkhardt, M. Boscolo, “Tools for Flexible Optimisation of IR Designs with Application to FCC”, IPAC 2015, these proceedings.
- [13] K. Ohmi, F. Zimmermann, “FCC-ee/CepC Beam-Beam Simulations with Beamstrahlung,” Proc. IPAC2014, p. 3766.
- [14] D. Shatilov, “Beam-Beam Effects in High-Energy Colliders: Crab Waist vs. Head-On,” Proc. ICFA HF2014, 9–12 October 2014, Beijing (2014).
- [15] A. Faus-Golfe, “Monochromatization for Higgs Production,” FCC Week 2015, Washington DC.
<http://indico.cern.ch/event/340703/session/-25/contribution/16/material/slides/1.pdf>
- [16] D. Shatilov, “Beam-Beam Optimization for FCC-ee at High Energies (120, 175 GeV),” FCC-ee video meeting, 11 December 2014.
<http://indico.cern.ch/event/333858/-contribution/1/material/slides/1.pdf>